

Optimum Gear Tooth Geometry for Minimum Fillet Stress Using BEM and Experimental Verification With Photoelasticity

Vasilios A. Spitas

Theodore N. Costopoulos¹

e-mail: cost@central.ntua.gr

Christos A. Spitas

Laboratory of Machine Elements,
National Technical University of Athens,
Iroon Politechniou 9,
15780, Athens, Greece

This paper introduces the concept of nondimensional gear teeth to be used in gear stress minimization problems. The proposed method of modeling reduces the computational time significantly when compared to other existing methods by essentially reducing the total number of design variables. Instead of modeling the loaded gear tooth and running BEA to calculate the maximum root stress at every iterative step of the optimization procedure, the stress is calculated by interpolation of tabulated values, which were calculated previously by applying the BEM on nondimensional models corresponding to different combinations of the design parameters. The complex algorithm is used for the optimization and the root stresses of the optimum gears are compared with the stresses of the standard gears for the same transmitted torque. Reduction in stress up to 36.5% can be achieved in this way. This reduction in stress has been confirmed experimentally with two-dimensional photoelasticity. [DOI: 10.1115/1.2216731]

Keywords: spur gears, root stress, BEM, optimization, complex algorithm, photoelasticity

1 Introduction

The advances in the field of computational mechanics and structural optimization have led to the development of numerical modeling techniques, which have been used in gearing applications to produce optimized designs of specific gear pairs (Litvin [1]). However, it is admitted (Ciavarella [2]) that since the design parameters of each individual gear are many, true real-time optimization requiring numerical stress analysis at every iterative step is practically impossible. In order to cope with this discrepancy, researchers resort to the use of empirical formulas (Pedrero [3]), or further simplify the problem by assuming loading at the tip of the tooth (Rogers [4]), yielding unreliable results when nonstandard teeth are studied.

This paper introduces a new concept in gear modeling by using the contact ratio of a gear pair for the determination of the point of load application. Instead of using the standard design parameters, the problem is simplified by using dimensionless teeth and by incorporating all the geometrical characteristics of the mating gear in the contact ratio of the pair, thus reducing the total number of parameters from seven to three. Each gear is thus geometrically modeled and consequently loaded at different points corresponding to different values of the contact ratio (ϵ) and subsequently B.E.A. follows to calculate the maximum root stress. The resultant values are tabulated in a "stress table" characterizing a given number of teeth, which can be readily included in an optimization algorithm, where all the required intermediate values can be quickly calculated by interpolation of the tabulated ones.

The new modeling technique offers improved accuracy and significantly smaller calculation times as opposed to the standard techniques employed. Moreover, owing to the concept of the "stress table," it can be readily synthesized in a modular way in any problem requiring the calculation of the maximum fillet

stress. Finally the results are verified using two-dimensional photoelasticity on polycarbonate plastic gear-tooth models.

2 Nondimensional Gear Tooth Modeling

Consider the pair of spur gears schematically illustrated in Fig. 1, where gear 1 is the pinion and gear 2 is the wheel. The law of gearing [5] requires that these gears should have the same nominal pressure angle α_o and the same module m in order to mesh properly. In the general case the gears are considered to have addendum modifications x_1, x_2 , respectively, i.e., and therefore, their pitch thickness is given by the following relationship:

$$s_{oi} = c_{si}m\pi + 2x_i m \tan \alpha_o = s_{oiu}m \quad (1)$$

where c_{si} is the thickness coefficient of gear i , ($i=1,2$), which in the general case is $c_{s1} \neq 0.5 \neq c_{s2}$, while s_{oiu} is the pitch thickness of the corresponding nondimensional gear for which the module (m) and the face width (b) are both equal to unity.

The center distance O_1O_2 is calculated using the following formula:

$$a_{12} = \frac{z_1 + z_2}{2}m + (x_1 + x_2)m = a_{12u}m \quad (2)$$

The actual operating pitch circle r_{bi} of gear i , ($i=1,2$) should verify the law of gearing and, therefore, be equal to

$$r_{bi} = \frac{z_i}{z_1 + z_2}a_{12u}m = r_{biu}m \quad (3)$$

Let us now consider gears 1 and 2 revolving about their centers O_1 and O_2 , respectively, and meshing along the path of contact AB as illustrated in Fig. 1. During meshing there are two pairs of gear teeth in contact along the segments AA' and BB' , thus sharing the total normal load, while there is only a single such pair when tooth contact takes place along the central region $A'B'$, carrying the total normal load. Point B' is the highest point of single tooth contact (HPSTC) for gear 1 and its position, defining the radius $r_{B'}$, is (Spitas [15])

¹Corresponding author.

Contributed by the Power Transmission and Gearing Committee of ASME for publication in the JOURNAL OF MECHANICAL DESIGN. Manuscript received March 9, 2005; final manuscript received November 27, 2005. Review conducted by Prof. David Dooner.

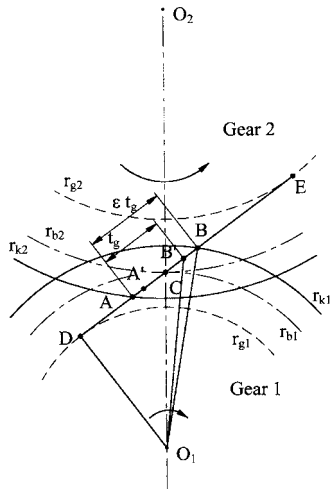


Fig. 1 Path of contact

$$r_{B'} = O_1B' = \sqrt{r_{k1}^2 + (\varepsilon - 1)t_g[(\varepsilon - 1)t_g - 2\sqrt{r_{k1}^2 - r_{g1}^2}]} \quad (4)$$

Dividing by the module of the pair, the above equation yields its equivalent in terms of nondimensional values

$$r_{B'u} = \frac{r_{B'}}{m} = \sqrt{r_{k1u}^2 + (\varepsilon - 1)t_{gu}[(\varepsilon - 1)t_{gu} - 2\sqrt{r_{k1u}^2 - r_{g1u}^2}]} \quad (5)$$

From the above equation it is evident that the position of the HPSTC of a gear depends only on its geometry and on the contact ratio of the pair, in which all the characteristics of the mating gear are incorporated in a condensed form.

The advantage offered by this approach is significant, since the mechanical behavior of every gear can be modeled only by using its own geometrical characteristics z, x, c_s and the contact ratio ε of the pair (four variables) instead of using all of the geometrical characteristics of the mating gear (six variables). Also the use of nondimensional teeth further simplifies the problem as every geometrical feature f on the transverse section of a full scale gear tooth is connected with the corresponding feature f_u of the transverse section of the nondimensional gear tooth through the equation

$$f = mf_u \quad (6)$$

Stresses can also be calculated in nondimensional teeth $\sigma_u(z, x, c_s, \varepsilon)$ with unit loading $P_{Nu}=1$ and related to the actual stress σ using the following equation:

$$\sigma = \sigma_u \frac{P_N}{bm} \quad (7)$$

as suggested by Rogers [4] and Townsend [5].

3 Stress Modeling Using Stress Tables

All the widely adopted analytical methods rely on the calculation of the nominal tensile bending stress at the fillet of the loaded spur gear tooth (Timoshenko [6]) and usually compensate for the stress concentration by introducing a stress concentration factor derived by either empirical or semiempirical methods. All standards treat the loaded gear tooth as a cantilever beam undergoing bending and the calculated nominal stress is multiplied by a stress concentration factor to produce the real bending stress.

According to the standard ISO 6336 [7], the nominal stress is calculated by using the assumption that the critical section lies at the point where a line with an inclination of 30 deg to the tooth centerline touches with the fillet internally. This has a tendency to overestimate the maximum fillet stress and has the disadvantage

of not considering the change of the critical section position due to the displacement of the load along the active tooth profile as suggested by Kelley and Pedersen [8].

The standard AGMA 2101-C95 [9] proposes a more detailed analytical approach to the problem, as it takes into consideration the change of the position of the critical section, which is considered to lie at the point where a parabola with its apex at the intersection of the load direction with the tooth centerline touches the fillet internally. This idea was introduced by Lewis [10] and, although it offers a better approach than the 30 deg theory, it can still introduce considerable errors, particularly if large tooth shifting is employed.

Simplified stress calculation methods are widely used in gear optimization problems (Rogers et al. [4], Yeh [11]), as the iterative methods used need a simple and yet efficient tool for gear stress modeling in order to diminish computational time for the thousands of iterations required. These do not take into account the geometry of the root fillet and the nominal stress is calculated by assuming only tip loading while neglecting the effect of bending stress concentration as well as of the compressive stress component.

Numerical methods such as F.E.M. and B.E.M. [1,2,12,13] have been successfully applied on loaded gear teeth offering increased accuracy and reliable stress estimation. The major disadvantage of these methods is that they require a lot of time for both the generation of the mesh and for the solution of the matrix equations. Furthermore they are difficult program and hence require the acquisition and use of sophisticated and expensive proprietary software.

The problems and shortcomings of the above methods can be overcome by the use of the "stress table" (see Table 1) in conjunction with the dimensionless tooth modeling presented in the previous paragraph. In order to create a stress table, a gear with a given number of teeth (z) is selected and then a range of possible addendum modification coefficients (x_{\min}, x_{\max}), tooth thickness coefficients ($c_{s\min}, c_{s\max}$), and contact ratios ($\varepsilon_{\min}, \varepsilon_{\max}$) is set. Each of these intervals is discretized in 4–6 values and for each combination (ε, x, c_s) the maximum dimensionless tensile stress $\sigma_u(\varepsilon, x, c_s)$ at the root fillet of the corresponding dimensionless tooth model is calculated through B.E.A. using quadratic isoparametric boundary elements. The calculation of the dimensionless tooth profile and the generation of the mesh are done automatically using specially developed software.

The results obtained by the analysis correspond to a single number of teeth are tabulated in a stress table characterizing the mechanical behavior of the gear. A representative table for 18 teeth has been calculated with the following characteristics: Nominal pressure angle $\alpha_o=20$ deg, Addendum coefficient $c_k=1.0$, Dedendum coefficient $c_j=1.25$, and Cutter radius coefficient $c_c=0.25$.

In order to calculate an intermediate stress value σ corresponding to a given number of teeth (z) and set of parameters z, x, c_s, ε not necessarily included in the stress table, linear interpolation is used as described below:

Step 1. From the stress table corresponding to the given tooth number the bounding values are chosen $\varepsilon_i \leq \varepsilon \leq \varepsilon_{i+1}$, $x_j \leq x \leq x_{j+1}$, $c_{sk} \leq c_s \leq c_{sk+1}$.

Step 2. From the stress table the stress values corresponding to the above bounding coefficient values are depicted:

$$\sigma(\varepsilon_i, x_j, c_{sk}) = \sigma_{i,j,k} \quad \sigma(\varepsilon_i, x_j, c_{sk+1}) = \sigma_{i,j,k+1} \quad (8)$$

$$\sigma(\varepsilon_i, x_{j+1}, c_{sk}) = \sigma_{i,j+1,k} \quad \sigma(\varepsilon_i, x_{j+1}, c_{sk+1}) = \sigma_{i,j+1,k+1} \quad (9)$$

$$\sigma(\varepsilon_{i+1}, x_j, c_{sk}) = \sigma_{i+1,j,k} \quad \sigma(\varepsilon_{i+1}, x_j, c_{sk+1}) = \sigma_{i+1,j,k+1} \quad (10)$$

$$\sigma(\varepsilon_{i+1}, x_{j+1}, c_{sk}) = \sigma_{i+1,j+1,k} \quad \sigma(\varepsilon_{i+1}, x_{j+1}, c_{sk+1}) = \sigma_{i+1,j+1,k+1} \quad (11)$$

Table 1 Stress table for 18 teeth

| $\epsilon=1.2$ | | | | | |
|--------------------|------------|------------|------------|------------|------------|
| $x \backslash c_s$ | $c_s=0.40$ | $c_s=0.45$ | $c_s=0.50$ | $c_s=0.55$ | $c_s=0.60$ |
| $x=-0.2$ | 5.730 | 4.818 | 4.141 | 3.621 | 3.211 |
| $x=+0.0$ | 4.965 | 4.246 | 3.696 | 3.262 | 2.912 |
| $x=+0.2$ | 4.502 | 3.887 | 3.406 | 3.021 | 2.708 |
| $x=+0.4$ | 4.032 | 3.510 | 3.094 | 2.758 | 2.484 |
| $x=+0.7$ | 3.729 | 3.257 | 2.873 | 2.561 | 2.306 |
| $\epsilon=1.4$ | | | | | |
| $x \backslash c_s$ | $c_s=0.40$ | $c_s=0.45$ | $c_s=0.50$ | $c_s=0.55$ | $c_s=0.60$ |
| $x=-0.2$ | 4.906 | 4.184 | 3.642 | 3.222 | 2.889 |
| $x=+0.0$ | 4.214 | 3.652 | 3.218 | 2.874 | 2.596 |
| $x=+0.2$ | 3.800 | 3.321 | 2.945 | 2.642 | 2.397 |
| $x=+0.4$ | 3.413 | 3.005 | 2.680 | 2.418 | 2.203 |
| $x=+0.7$ | 3.054 | 2.702 | 2.415 | 2.183 | 1.993 |
| $\epsilon=1.6$ | | | | | |
| $x \backslash c_s$ | $c_s=0.40$ | $c_s=0.45$ | $c_s=0.50$ | $c_s=0.55$ | $c_s=0.60$ |
| $x=-0.2$ | 4.391 | 3.793 | 3.339 | 2.986 | 2.703 |
| $x=+0.0$ | 3.741 | 3.283 | 2.927 | 2.643 | 2.412 |
| $x=+0.2$ | 3.282 | 2.911 | 2.618 | 2.382 | 2.189 |
| $x=+0.4$ | 2.942 | 2.629 | 2.380 | 2.177 | 2.012 |
| $x=+0.7$ | 2.602 | 2.339 | 2.125 | 1.952 | 1.809 |
| $\epsilon=1.8$ | | | | | |
| $x \backslash c_s$ | $c_s=0.40$ | $c_s=0.45$ | $c_s=0.50$ | $c_s=0.55$ | $c_s=0.60$ |
| $x=-0.2$ | 3.978 | 3.485 | 3.109 | 2.812 | 2.573 |
| $x=+0.0$ | 3.356 | 2.990 | 2.703 | 2.472 | 2.284 |
| $x=+0.2$ | 2.928 | 2.640 | 2.411 | 2.225 | 2.072 |
| $x=+0.4$ | 2.616 | 2.379 | 2.188 | 2.033 | 1.904 |
| $x=+0.7$ | 2.253 | 2.070 | 1.921 | 1.800 | 1.699 |

Step 3. The following intermediate stress values are calculated:

$$\sigma_{i,j} = \sigma_{i,j,k} + \frac{\sigma_{i,j,k+1} - \sigma_{i,j,k}}{c_{sk+1} - c_{sk}}(c_s - c_{sk})$$

$$\sigma_{i,j+1} = \sigma_{i,j+1,k} + \frac{\sigma_{i,j+1,k+1} - \sigma_{i,j+1,k}}{c_{sk+1} - c_{sk}}(c_s - c_{sk})$$

$$\sigma_{i+1,j} = \sigma_{i+1,j,k} + \frac{\sigma_{i+1,j,k+1} - \sigma_{i+1,j,k}}{c_{sk+1} - c_{sk}}(c_s - c_{sk}) \quad (12)$$

$$\sigma_{i+1,j+1} = \sigma_{i+1,j+1,k} + \frac{\sigma_{i+1,j+1,k+1} - \sigma_{i+1,j+1,k}}{c_{sk+1} - c_{sk}}(c_s - c_{sk}) \quad (13)$$

$$\sigma_i = \sigma_{i,j} + \frac{\sigma_{i,j+1} - \sigma_{i,j}}{x_{j+1} - x_j}(x - x_j)$$

$$\sigma_{i+1} = \sigma_{i+1,j} + \frac{\sigma_{i+1,j+1} - \sigma_{i+1,j}}{x_{j+1} - x_j}(x - x_j) \quad (14)$$

Step 4. The desired stress is calculated as:

$$\sigma(z, \epsilon, x, c_s) = \sigma_i + \frac{\sigma_{i+1} - \sigma_i}{\epsilon_{i+1} - \epsilon_i}(\epsilon - \epsilon_i) \quad (15)$$

The increments of the parameters z, x, c_s, ϵ used in the stress tables were selected so that the maximum interpolation error is kept below 1.2%. This is in good accordance with the overall accuracy of the analytical methods employed in calculating the stress values, therefore, a tighter selection of increments will not result in a tangible increase in stress prediction accuracy.

4 Formulation of the Objective Function

Analytical optimization methods are not suitable for gear stress optimization problems due to the complex implicit functions that relate the main geometrical variables to the resulting stresses. An efficient method of solving such intricate problems is the Complex algorithm [14], which calculates the minimum of a function of n variables $f(\mathbf{x})$, where $\mathbf{x}=(x_1, x_2, \dots, x_n)^T$ is the variable vector.

In any gear pair the maximum tensile stresses developed at the root fillet of each tooth are not equal but usually in unshifted gears the stress developed at the pinion is greater than that developed on the wheel. It is also established (Townsend [5]) that the root stress is maximized when the tooth mates at its HPSTC because the applied normal load to the profile and its leverage to the critical section reach their maximum values. Therefore, the objective of gear tooth optimization is to reduce the maximum stress at both fillets assuming loading at the HPSTC.

The independent variables of a stress optimization problem considering nondimensional gears are the following:

Addendum modifications: x_1 for gear 1 x_2 for gear 2

Thickness coefficients: c_{s1} for gear 1 c_{s2} for gear 2

The objective function without any constraints is defined as:

$$\min f(x_1, x_2, c_{s1}, c_{s2}) = \max(\sigma_1, \sigma_2)$$

where σ_1, σ_2 are the maximum tensile stresses developed at the fillets of the conjugate gears 1 and 2, respectively, when loaded at their corresponding HPSTC.

Naturally, the optimization must be constrained because the optimum teeth should still fulfill certain operational criteria. There are seven different constraints described below and in order to

include them in the optimization procedure the following form of the objective function is adopted using weighted residuals:

$$\min f(x_1, x_2, c_{s1}, c_{s2}) = \max(\sigma_1, \sigma_2) + \sum_{i=1}^7 w_i c_i \quad (16)$$

The penalty functions c_i and the weighting coefficients w_i employed in Eq. (16) are defined below. In general, the penalty functions either take arbitrarily big values when variables exceed the permissible design boundaries in order to exclude them from the next iterative steps, or are related to the actual variable values in order to facilitate smooth convergence. In the latter case the values of the weighting coefficients are chosen as to provide products $w_i x_i$ comparable to the nondimensional stresses within the objective function and thus streamlining the process.

Constraint 1: Allowable addendum modification: The addendum modification coefficient for gear i is restricted between two values $x_{i\min}$ and $x_{i\max}$ depending on the number of teeth z . These values are dictated by common gear practice and manufacture. In each stress table there is a range of addendum modification coefficients that must not be exceeded, or fatal errors during the execution of the program occur. If x_i in the complex vector lies beyond the allowable range, the penalty functions and weighting coefficients take sufficiently big values (i.e., 1000 which is at least two orders of magnitude higher than the expected optimum solutions) in order to exclude them from the next iteration and if they lie within the range, the penalty is equal to zero, therefore:

$$\begin{aligned} &\text{If } x_i < x_{i\min} \text{ or } x_i > x_{i\max}, i=1,2 \text{ then } w_1 c_1 = 1000, \sigma_1 = \sigma_2 = 1000; \\ &\text{If } x_{i\min} \leq x_i \leq x_{i\max}, \text{ for every } i=1,2 \text{ then } w_1 c_1 = 0. \end{aligned}$$

Constraint 2: Allowable thickness coefficients: For technical reasons the cutting tool producing the gears (rack cutter, pinion cutter or hob) cannot have infinitely thick or infinitely thin teeth and this imposes a constraint on the resulting thickness of the produced gear. Therefore the thickness coefficient should range between the values $c_{s\min}$ and $c_{s\max}$, which are the limit values specified in the stress tables. As in constraint 1, in order to exclude values which lie beyond the allowable limits, the penalty function assumes the value of 1000 and 0 when the values of c_{si} lie within the limits, hence:

$$\begin{aligned} &\text{If } c_{si} < c_{si\min} \text{ or } c_{si} > c_{si\max}, i=1,2 \text{ then } w_2 c_2 = 1000, \sigma_1 = \sigma_2 = 1000; \\ &\text{if } c_{si\min} \leq c_{si} \leq c_{si\max}, \text{ for every } i=1,2 \text{ then } w_2 c_2 = 0. \end{aligned}$$

Constraint 3: Minimum radial clearance: In order to ensure that the conjugate gears operate without the risk of seizure, there should be a minimum allowable radial clearance $c_{r\min} \cdot m$, where $c_{r\min} = 0.25$. For the dimensionless gear i it is calculated from the equation:

$$\begin{aligned} c_{ri} &= a_{12} - r_{kiu} - r_{fii} = c_f - c_k = c_r, \\ \text{where } r_{uki} &= \frac{z_i}{2} + x_i + c_k \quad \text{and} \quad r_{ufi} = \frac{z_i}{2} + x_i - c_f \end{aligned}$$

are the tip and root radius of the nondimensional gear i and $c_k = 1.0$, $c_f = 1.25$ are the addendum and dedendum coefficients, respectively. The penalty functions are thus formulated: If $c_r < 0.25$ then $c_3 = 0.25 - c_r$ and $w_3 = 10$.

Here the penalty function c_3 has been chosen to be a function of the radial clearance in order to help the convergence of the solution at points where the nondimensional coefficient c_r approaches its nominal value of 0.25. The value of the weighting coefficient was chosen equal to 10 in order to improve the convergence of the algorithm.

If $c_r > 0.25$ then $w_3 c_3 = 0$.

Constraint 4: Interference: If the tip radius r_{ki} of gear i revolving about O_i exceeds a maximum value $r_{ki\max}$ so that the inter-

section of the tip circle of the gear with the common path of contact at point U defines on the mating gear j a radius which is lower than its form radius r_{js} , then interference occurs, since the tooth part below the form radius has a trochoidal and not an involute form. Consequently, it should always be $r_{ki} \leq r_{ki\max}$, where $r_{ki\max} = O_i U$. In terms of the corresponding dimensionless gears this results in the following penalty function:

$$\begin{aligned} &\text{If } r_{kiu} > r_{ki\max}, i=1,2 \text{ then } c_4 = \max(r_{k1u} - r_{k1\max}, r_{k2u} - r_{k2\max}) \text{ and } w_4 = 5; \\ &\text{if } r_{kiu} \geq r_{ki\max} \text{ for every } i=1,2 \text{ then } w_4 c_4 = 0. \end{aligned}$$

Constraint 5: Minimum tip thickness: In common gear practice the tip thickness is never below 0.2 times the module or tip fracture would occur. In a nondimensional gear the tip thickness should always be $s_{ku} \geq 0.2$.

$$\begin{aligned} &\text{If } s_{kui} < 0.25, i=1,2 \text{ then } c_5 = \min(s_{k1}, s_{k2}) \text{ and } w_5 = 10; \\ &\text{if } s_{kui} \geq 0.25 \text{ for every } i=1,2 \text{ then } w_5 c_5 = 0. \end{aligned}$$

Constraint 6: Allowable contact ratio: In order to ensure smooth and unproblematic running the contact ratio of a gear pair should exceed 1.2. A usual upper limit is 1.8, which in 20 deg standard or shifted spur gears is never surpassed. Similarly to the constraints 1 and 2 the contact ratio ϵ of the pair should lie in the range defined in the stress tables, therefore, big penalties are applied at the boundaries:

$$\begin{aligned} &\text{If } \epsilon < \epsilon_{\min} \text{ or } \epsilon > \epsilon_{\max} \text{ then } w_6 c_6 = 1000, \sigma_1 = \sigma_2 = 1000; \\ &\text{if } \epsilon_{\min} \leq \epsilon \leq \epsilon_{\max} \text{ then } w_6 c_6 = 0. \end{aligned}$$

Constraint 7: Allowable backlash: The backlash of a gear pair (B) should always be positive and usually optimized designs require that this is kept minimum since the thicker the working teeth are, the less the root stress is. Although zero backlash is never actually desirable for power transmissions, the presence of a minimum backlash does not seriously reduce the tooth thickness, hence the root stresses and, therefore, in order to simplify the calculations the optimum backlash can be considered zero. This can be expressed in terms of a penalty function, suitably big beyond the permissible boundaries, as

$$c_7 = B \quad \text{and} \quad w_7 = 1000.$$

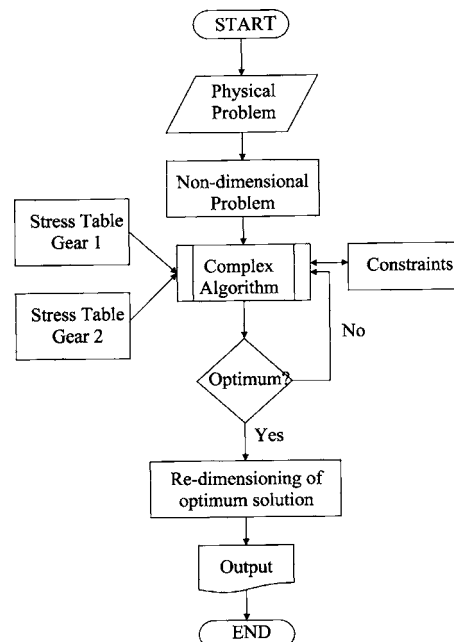


Fig. 2 The optimization algorithm

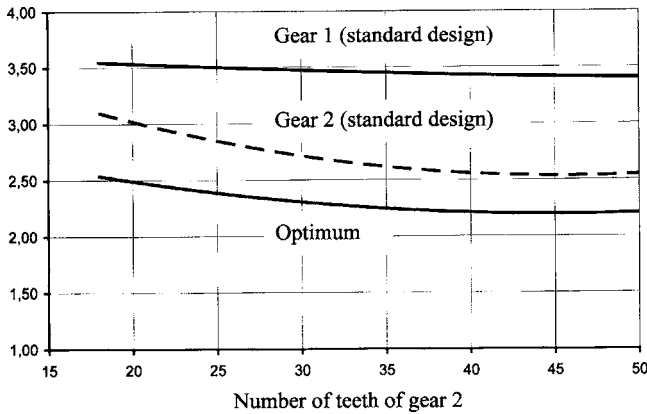


Fig. 3 Nondimensional root stress for $z_1=12$ pinion teeth

After the formulation of the objective function the algorithm described in Fig. 2 is executed.

5 Results and Discussion

The optimization method described above has been implemented on various combinations of a 20 deg involute pinion with 12 teeth meshing with gears having 15, 18, 22, 28, and 50 teeth. The stress tables were first constructed for all the above-described numbers of teeth and for the optimization algorithm the following parameter values were used: $\epsilon=1 \times 10^{-4}$ (tolerance), $\alpha=1.2$ (reflection coefficient), $\beta=1.0$ (expansion coefficient), $\gamma=2.0$ (contraction coefficient). The parameter values were chosen so as to provide quick convergence and stability of the algorithm.

In Fig. 3 the values of the maximum root stress for the nondimensional pinion with 12 teeth and its conjugate gears with 18–50 teeth are plotted. In this figure it can be observed that the maximum pinion stress (gear 1) is always greater than the maximum stress on the mating wheel (gear 2) in the case of standard gears while these stresses are equal in the case of optimized gears. In Fig. 4 the percent reduction of the maximum root stress offered by the optimum design is plotted for pinion teeth equal to 12 and gear teeth from 18 to 50. The maximum reduction in the fillet stress is achieved for a pinion with 12 teeth and a gear with 50 teeth and reaches 36.5%.

The total computational time is 95 s on a 1.6 GHz Pentium IV based system. The optimization algorithm used a complex of $m=1000$ vectors and reached the optimum solution after $i=29$ iterations performing over 40,000 stress calculations. By following the

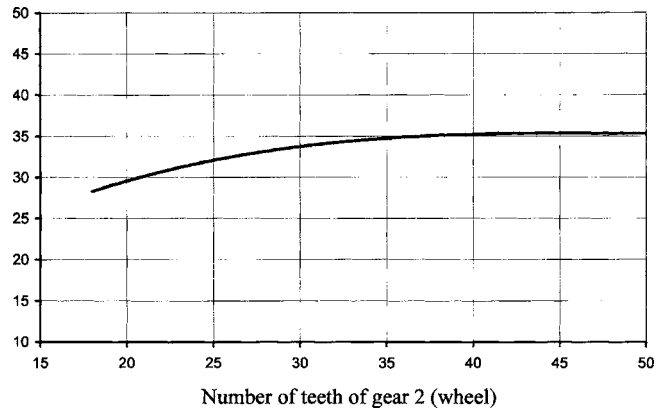


Fig. 4 (%) Reduction of the root stress for optimum gears (pinion with 12 teeth)

standard methodology performing full gear modeling (run time 1.6 s), mesh generation (run time 0.4 s) and BEA (run time 19 s) at each iterative step, this would result in a total run time of more than $40,000 \times (1.6+0.4+19)=840,000$ s or 233 h, which is too much.

The optimum design has been experimentally verified using two-dimensional photoelasticity [15]. The specimens corresponded to shifted involute gear teeth and they were made of special polycarbonate material. The fillet stresses were experimentally measured on a circular plane polariscope under both white and monochromatic sodium light. The loading was exerted on the specimen with a specially designed mechanism in order to ensure that the load is always normal to the profile and that frictional forces are not present. The photoelastic study included not only the optimum specimens but also specimens corresponding to the nominal (unshifted) teeth and teeth cut according to other standards for comparison. The experimental results are in excellent agreement with the numerical predictions (maximum deviation of 3.6%) and the new design offers a decrease of the maximum fillet stress ranging from 13.5% to 36.5% depending on the geometrical characteristics of the gear pair. The measured difference between the pinion and the gear fillet stress never exceeds 1.8%.

In Fig. 5 three different pinion tooth specimens correspond to a 28-tooth pinion / 50-tooth wheel pair. The left tooth design is the proposed optimum geometry, the central tooth corresponds to the AGMA standard recommendation for minimum fillet stress and the right is according to the FZG recommendation for minimum

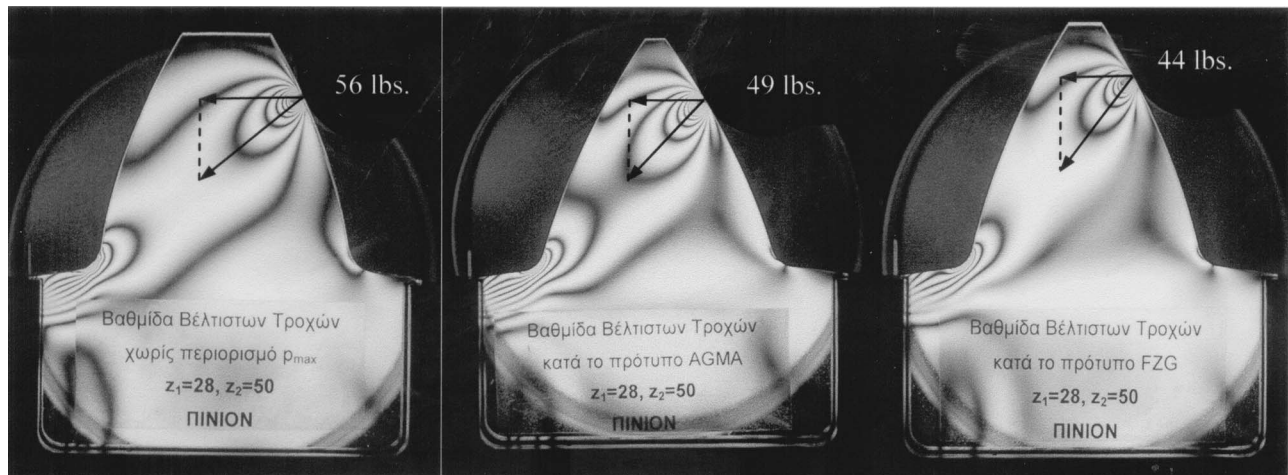


Fig. 5 Photoelastic fringe patterns on sample gear-tooth models

fillet stress. All specimens are loaded at their HPSTC with progressively increasing normal load until a third-order isochromatic fringe appears at the root fillet critical section, meaning that all specimens develop the same principal (maximum tensile) stress at that point. From the experiment it is easily deduced that the load-bearing capacity of the optimum design is increased by 14% compared to the AGMA recommendation and by 27% compared to the FZG recommendation.

This technique has been already successfully incorporated in a number of gear optimization problems and its results are in good agreement with photoelastic investigations [15].

6 Conclusions

In this paper the concepts of the nondimensional gears and the stress tables have been introduced and used for gear stress optimization with the Complex algorithm. The nondimensional gears are used in order to decrease the total number of the optimization parameters by introducing the contact ratio of the pair as the parameter defining completely the point of loading. This reduction in the number of parameters enabled the tabulation of the maximum root stress developed on each nondimensional gear with a given number of teeth for different values of addendum modification, pitch thickness and contact ratio using BEM. During the iterative optimization procedure, the stress values for different combinations of the geometrical parameters of the conjugate gears of the pair were calculated from interpolation of the tabulated values at high speed and with satisfactory accuracy. In this way, the run time decreased dramatically (in the order of 8000 times) compared to the standard approach without any effect on the accuracy.

Therefore, the proposed modeling provides the design engineer with a fast, productive, reliable, and easy to implement tool for solving gear stress optimization problems and calculating gear stresses at cases not covered satisfactorily by the existing standards.

Nomenclature

Gear Description

| | | |
|---------------|---|------------------------------|
| α_o | = | pressure angle |
| a_{12} | = | center distance |
| b | = | tooth width |
| c_c | = | cutter radius coefficient |
| c_f | = | dedendum coefficient |
| c_k | = | addendum coefficient |
| c_s | = | thickness coefficient factor |
| ε | = | contact ratio |
| m | = | module |
| P_N | = | normal force |
| r_b | = | operating pitch radius |
| r_g | = | involute base radius |
| r_k | = | outside radius |

| | | |
|----------|---|--|
| σ | = | bending stress at tooth critical cross section |
| s_o | = | tooth thickness at pitch circle |
| t_g | = | base pitch |
| x | = | addendum modification coefficient |
| z | = | number of teeth |

Indices

| | | |
|-----|---|-----------------------------|
| u | = | ref. to nondimensional gear |
| i | = | ref. to gear no. i |

Optimization

| | | |
|--------------|---|----------------------------------|
| f | = | objective function |
| \mathbf{x} | = | vector of optimization variables |
| c | = | penalty function |
| w | = | weighting coefficient |

Complex Algorithm

| | | |
|------------|---|-------------------------|
| ϵ | = | tolerance |
| α | = | reflection coefficient |
| β | = | expansion coefficient |
| γ | = | contraction coefficient |

References

- [1] Litvin, F. L., Qiming, L., and Kapelvich, A. L., 2000, "Asymmetric Modified Spur Gear Drives Reduction of Noise, Localization of Contact, Simulation of Meshing and Stress Analysis," *Comput. Methods Appl. Mech. Eng.*, **188**, pp. 363–390.
- [2] Ciavarella, M., and Demelio, G., 1999, "Numerical Methods for the Optimization of Specific Sliding, Stress Concentration and Fatigue Life of Gears," *Int. J. Fatigue*, **21**, pp. 465–474.
- [3] Pedrero, J. I., Rueda, A., and Fuentes, A., 1999, "Determination of the ISO Tooth Form Factor for Involute Spur and Helical Gears," *Mech. Mach. Theory*, **34**, pp. 89–103.
- [4] Rogers, C. A., Mabie, H. H., and Reinholtz, C. F., 1990, "Design of Spur Gears Generated with Pinion Cutters," *Mech. Mach. Theory*, **25**(6), pp. 623–634.
- [5] Townsend, D. P., 1992, *Dudley's Gear Handbook*, McGraw-Hill, New York.
- [6] Timoshenko, S., and Baud, R. V., 1926, "Strength of Gear Teeth," *Mech. Eng. (Am. Soc. Mech. Eng.)*, **48**, 1105–1109.
- [7] ISO, 1996, "Calculation of the Load Capacity of Spur and Helical Gears-Part 3: Calculation of Tooth Bending Strength," ISO Paper No. ISO 6336-3:1996.
- [8] Kelley, B. W., and Pedersen, R., 1950, "The Beam Strength of Modern Gear Tooth Design," *SAE Trans.*, **66**, pp. 360–367.
- [9] American Gear Manufacturers Association, 1995, "Fundamental Rating Factors and Calculation Methods for Involute Spur and Helical Gear," Paper No. AGMA 2101-C95.
- [10] Lewis, W., 1882, "Investigation of Strength of Gear Teeth," *Proceedings of the Engineering Club No. 1*, Philadelphia, pp. 16–23.
- [11] Yeh, T., Yang, D., and Tong, S., 2001, "Design of New Tooth Profiles for High-Load Capacity Gears," *Mech. Mach. Theory*, **36**, pp. 1105–1120.
- [12] Andrews, J., 1991, "A Finite Element Analysis of Bending Stresses Included in External and Internal Involute Spur Gears," *J. Strain Anal. Eng. Des.*, **26**(3), pp. 153–163.
- [13] Spitas, V. A., and Costopoulos, T., "New Concepts in Numerical Modeling and Calculation of the Maximum Root Stress in Spur Gears Versus Standard Methods. A Comparative Study," *Proceedings 1st National Conference on Recent Advances in Mech. Eng., Patras*, ANGI/P106, 2001.
- [14] Box, M. J., 1965, "The Complex Algorithm," *Computer*, **8**, pp. 42–52.
- [15] Spitas, V., 2001, "Modeling and Design of Optimum Gears Using Analytical, Numerical and Experimental Methods," Ph.D. thesis, National Technical University of Athens, Greece.